

Carbon-covered Alumina: A Superior Support of Noble Metal-like Catalysts for Hydrazine Decomposition

Mingyuan Zheng · Yuying Shu · Jun Sun ·
Tao Zhang

Received: 24 July 2007 / Accepted: 4 October 2007 / Published online: 20 October 2007
© Springer Science+Business Media, LLC 2007

Abstract Carbon-covered alumina (CCA) were synthesized from mesoporous alumina and a series of carbon sources (including sucrose, furfuryl alcohol, and benzene). They had structural properties of alumina and surface characteristics of carbon. When they were used as supports for molybdenum carbide, nitride, and phosphide catalysts, significantly higher activities were obtained in hydrazine decomposition as compared to those supported on the conventional alumina. The difference in the interactions of catalytic active sites with the CCA and with the alumina supports was preliminarily deemed to be the main cause of the better performance of CCA supported catalysts. Carbon contents on alumina and carbon sources were found to be important for CCA to be a good support. Carbon deposited on alumina in a near monolayer form showed the best activities. In contrast with sucrose and furfuryl alcohol, benzene as the carbon source readily yielded CCA supports with a hydrophobic surface, which resulted in relatively low dispersions of metal and, in turn, decreased activity of the supported catalysts.

Keywords Hydrazine decomposition · Carbon covered alumina · Carbide · Nitride · Phosphide

1 Introduction

Hydrazine catalytic decomposition has important applications in attitude control of spacecrafts, in which Ir/Al₂O₃ is usually used as a catalyst. Transition metal interstitial compounds, including carbides, nitrides, and phosphides, behave noble metal-like in many reactions involving hydrogen transfer [1–3]. They have been found to be promising substitutes for the rare and expensive iridium in N₂H₄ decomposition [4–6]. For instance, the supported catalysts Mo₂C/Al₂O₃ and Mo₂N/Al₂O₃ reported by Chen et al. showed high performances in hydrazine thrusters at 100 °C [7, 8]. However, at lower temperatures, these noble metal-like catalysts presented activities needing further improvement for future applications.

Support is very important for a catalyst, as the support determines the catalytic performance from micro and macro aspects. This is especially true for hydrazine decomposition. In this process catalysts endure high temperature, high pressure, and rapid flushing with reactant and products at high velocities. Alumina has been conventionally used as a support for this reaction due to its various advantages in terms of high surface areas, numerous pores, and strong mechanical strength. On the other hand, it also has some potentially detrimental characteristics. For example, its strong interactions with metal atoms might cause a decrease in catalytic activity. The acidic surface could adsorb N₂H₄ and cause catalyst deterioration under working conditions in thrusters.

A carbon support has many properties different from alumina, such as mild interactions with supported metals, a neutral surface, and good thermal conductivity. It is likely that these properties might enable carbon-supported catalysts to perform better than their alumina counterparts. Furthermore, when carbon is used as a support for

M. Zheng · Y. Shu · J. Sun · T. Zhang (✉)
Dalian Institute of Chemical Physics, Chinese Academy
of Sciences, Dalian 116023, China
e-mail: taozhang@dicp.ac.cn

Y. Shu
e-mail: yyshu@dicp.ac.cn

transition metal carbide catalysts, the catalysts can be prepared by a temperature-programmed reaction in a hydrogen flow. In such an atmosphere the carbon support provides the carbon source for the carburization. This can efficiently suppress the formation of detrimental carbonaceous deposits on the surface of the carbide, which usually occurs when the carburization proceeds in a CH_4/H_2 atmosphere [9]. Unfortunately, difficulties in controlling the pore sizes of the carbon have hindered its utilization as a catalyst support for N_2H_4 decomposition. For example, the micropores in the active carbon will allow the carbon supported catalyst to be readily crushed.

Carbon-covered alumina (CCA) retains the structure and physical characteristics of alumina while having a similar, but carbonaceous, surface. Consequently, some properties from both the alumina and the carbon are integrated onto the CCA, and it is reasonable to assume that this might make CCA supported catalysts show superior catalytic properties. In this work, CCA supports were prepared from several carbon sources and then used for the noble metal-like catalysts, including molybdenum carbide, nitride, and phosphide. The catalysts were compared with those supported on alumina in hydrazine decomposition. The influences of the carbon contents and carbon sources on the activities of catalysts were also discussed.

2 Experimental

2.1 CCA Supports Preparation

CCA-S supports were prepared by using sucrose as the carbon source as reported by Lin et al. [10]. In detail, 2.0 g alumina (homemade, 20–40 mesh) was impregnated to incipient wetness with an aqueous solution of sucrose (weight ratio of sucrose/ Al_2O_3 was 0.4:1, 0.5:1, and 0.6:1, respectively), dried at 90 °C, and then calcined in flowing N_2 (100 mL/min) with a 400 min ramp and with a 60 min hold at 800 °C (denoted as CCA-S-0.4, CCA-S-0.5, and CCA-S-0.6, respectively). CCA-B supports were prepared from benzene by chemical vapor deposition [11], i.e., 2.0 g alumina was heated in flowing $\text{C}_6\text{H}_6/\text{N}_2$ (100 mL/min, benzene vapor saturated at 27 °C) with a 70 min ramp and with a hold at 725 °C for 1 h, 2 h, and 3 h, respectively (denoted as CCA-B-1, CCA-B-2, and CCA-B-3, respectively), followed by a N_2 purge for 30 min at the preparation temperature and then allowed to cool down to room temperature. CCA-F support was prepared from furfuryl alcohol. In detail, 2.0 g alumina was impregnated to incipient wetness with furfural alcohol at room temperature and then polymerized at 95 °C for 12 h. The derived sample was calcined with a 400 min ramp and 1 h hold at 800 °C under pure N_2 atmosphere (100 mL/min).

2.2 Catalysts Preparation

2.2.1 Molybdenum Carbide Catalysts

The various CCA supports were impregnated to incipient wetness with an aqueous solution of ammonia molybdate and dried at 120 °C for 12 h. The samples were then carburized in flowing H_2 with a three-stage heating procedure: from room temperature to 300 °C in 30 min, then to 700 °C at a rate of 1 °C/min, and finally kept at 700 °C for 1 h. The as-prepared carbide catalysts were passivated with 1 vol.% O_2/N_2 at room temperature for 8 h to prevent fierce oxidation upon exposure to air. For comparison, an alumina-supported molybdenum carbide catalyst ($\text{Mo}_2\text{C}/\text{Al}_2\text{O}_3$) and an active carbon-supported catalyst ($\text{Mo}_2\text{C}/\text{AC}$, active carbon from Norit Company) were also prepared. The preparation procedures were similar to those of $\text{Mo}_2\text{C}/\text{CCA}$, except for a further calcination of $\text{MoO}_3/\text{Al}_2\text{O}_3$ at 450 °C in air after drying at 120 °C, and the carburization in H_2/CH_4 (20 vol.%) for the $\text{Mo}_2\text{C}/\text{Al}_2\text{O}_3$ catalyst. The Mo metal loadings on various supports were all 12.0 wt.%.

2.2.2 Molybdenum Nitride Catalysts

Molybdenum nitride catalysts supported on CCA-S-0.5 and Al_2O_3 (20–40 mesh) were prepared with processes similar to those of the molybdenum carbide catalysts mentioned above, except the preparation atmosphere was changed from H_2 or CH_4/H_2 to pure NH_3 . The Mo metal loadings were also 12.0 wt.%.

2.2.3 Phosphide Catalysts

2.0 g CCA-S-0.5 support was impregnated to incipient wetness with a solution of ammonia molybdate and $(\text{NH}_4)_2\text{HPO}_4$ (mol ratio of Mo:P = 1:1.1) then dried at 120 °C for 12 h in air and calcined at 500 °C for 2 h in flowing N_2 . The following reduction was performed at 700 °C for 2 h in a pure H_2 flow to yield supported molybdenum phosphide catalyst. For comparison, $\text{MoP}/\text{Al}_2\text{O}_3$ was prepared by a similar procedure, except the calcination of the precursor was under an air atmosphere, and the reduction temperature was 750 °C. The Mo loadings of these two catalysts were both 12.0 wt.%.

2.3 Catalyst Characterization

The Brunauer-Emmett-Teller (BET) surface areas (S_{BET}), pore volumes, and pore size distributions were measured by the N_2 adsorption at -196 °C on a volumetric adsorption

unit (Micromeritics ASAP 2010). The XRD patterns of samples were obtained on a Rigaku D/MAX- β B diffractometer operated at 40 kV and 100 mA, using Cu $k\alpha$ monochromatized radiation. The carbon contents on the CCA supports were measured by a TG-DTA thermal analyzer (Setram Setsys TMA 16/18).

UV Raman spectroscopy was carried out on a Jobin Yvon S. A. T64000 triple-stage spectrometer equipped with three 2,400 grooves/mm gratings and a specially coated UV-sensitive CCD detector. A line at 325 nm from a He-Cd laser was used as the excitation source. The spectra were recorded by using a 180° geometry with a laser power of about 3 mW on the sample to avoid damaging the sample. Each spectrum was collected for 300 s.

2.4 Evaluation of Catalysts for Hydrazine Decomposition

The catalysts were evaluated in a fix-bed reactor as described elsewhere [5, 6]. About 0.1 g catalyst (20–40 mesh) was mixed with quartz granules (0.2 g, 20–40 mesh) and loaded in a U-shaped quartz reactor (i.d. 5 mm). Feedstock ($\text{N}_2\text{H}_4/\text{Ar}$, ~ 3 v/v%) was maintained at a rate of 85 mL/min. The products N_2 , H_2 , and NH_3 , as well as unreacted hydrazine, were analyzed with an on-line chromatograph (Agilent 6890) equipped with a TCD detector.

3 Results and Discussion

3.1 Characterization Results

The N_2 adsorption-desorption isotherms of CCA and alumina supports are shown in Fig. 1. CCA-S-0.5, CCA-B-1, and CCA-F had N_2 adsorption-desorption isotherms similar to those of Al_2O_3 , which indicates that the original pore structure of alumina was well retained after the surface was covered with carbon. This was in accordance with work

reported by Lin et al. [10]. Figure 1b presents the pore size distribution curves of these supports from the desorption branches of isotherms according to the BJH (Barrett-Joyner-Halenda) method. Al_2O_3 had pore diameters centered at 5.3 nm. The CCA-F, CCA-S-0.5, and CCA-B-1 had pore diameters centered at lower values, i.e., ca. 4.7 nm–3.8 nm, suggesting that carbon species occupied the inner surface of the alumina pores and caused some decrease in the pore sizes.

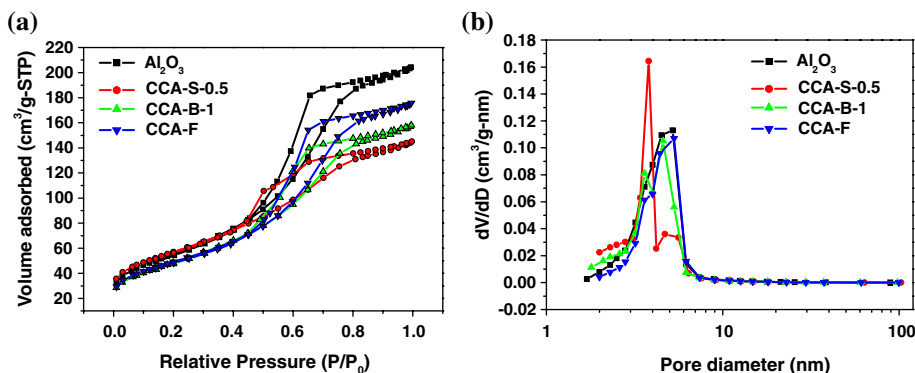
More detailed textural parameters of various supports are listed in Table 1. CCA-B-1 and CCA-F had surface areas very close to that of Al_2O_3 -800 (vacant alumina, calcined at 800 °C as CCA-S), demonstrating that the high surface areas of alumina were well retained on these CCA supports. CCA-S-0.5 even had a slightly higher surface area than that of Al_2O_3 -800, which can be attributed to the formation of carbon with micropores. When sucrose was impregnated onto an alumina support, it readily crystallized during the drying process and further produced coke with micropores in the following pyrolysis.

The average diameters of CCA-F, CCA-B-1, and CCA-S-0.5 were lower than that of Al_2O_3 -800 by 0.2–0.8 nm. Since the thickness of monolayer graphitized carbon is 0.34 nm, the diameter of a cylindrical pore will decrease by ca. 0.68 nm when its inner surface is covered with one layer of carbon. Accordingly, it can be inferred that CCA-S-0.5 and CCA-B-1 might be deposited with carbon in a

Table 1 Texture properties of CCA, active carbon (AC), and alumina supports

Supports	Temp. (°C)	S_{BET} (m^2/g)	D (nm)	S_{mic} (m^2/g)	V (cm^3/g)	Carbon content (%)
Al_2O_3	450	202	4.6	0	0.32	0
Al_2O_3 -800	800	186	4.9	0	0.32	0
CCA-S-0.5	800	204	4.1	17	0.24	11.4
CCA-B-1	725	177	4.3	0	0.25	9.2
CCA-F	800	178	4.7	8	0.28	4.1

Fig. 1 N_2 adsorption-desorption isotherms (a) and pore size distributions (b) of various supports derived from the N_2 desorption branch of isotherm by the BJH method



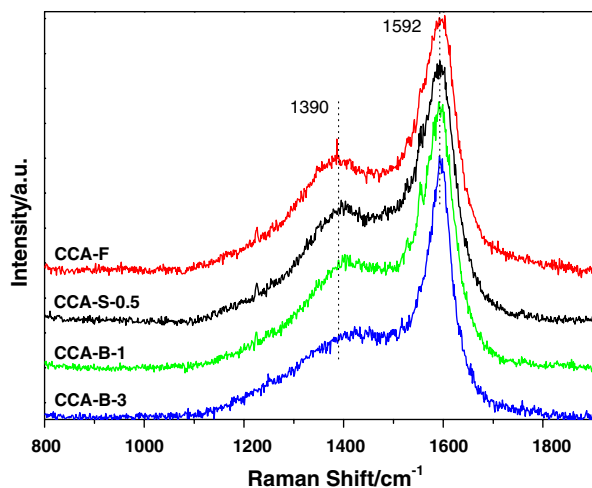


Fig. 2 UV Raman spectra of samples CCA-S-0.5, CCA-F, and CCA-B-1

nearly continuous monolayer, whereas the coverage of carbon on CCA-F must be much less continuous.

The carbon contents obtained by TG-DTA analysis (listed in Table 1) revealed the apparent difference in the carbon coverage on these CCA supports. For the Al_2O_3 whose surface is entirely covered by a single layer of graphitized carbon, the calculated carbon content is about 12.4 wt.%. Therefore, the carbon coverage on CCA-F would be less than 30% of a monolayer on the alumina surface, whereas the carbon coverage on CCA-S-0.5 and CCA-B-1 might be near 100%.

Figure 2 shows the UV Raman spectra of CCA supports. Two peaks at 1390 cm^{-1} and 1592 cm^{-1} were observed and denoted as peaks D and G, respectively, and they are due to the sp^2 carbon species. According to Ferrari et al. [12, 13], the D peak is related to the breathing modes of sp^2 carbon atoms in rings, and the G peak comes from the bond stretching of all pairs of sp^2 carbon atoms in both rings and chains. The calculations showed that the ratio of $I(\text{D})/I(\text{G})$ (intensity ratio of the D peak to the G peak) for CCA-B-3 was 0.32 and lower than the ratios of 0.41 for the CCA-B-1, CCA-S-0.5, and CCA-F. This indicates that the carbon species deposited on CCA-B-3 were graphite grains with larger size as compared to those on CCA-B-1, etc.

Figure 3 shows the XRD patterns of the molybdenum carbide supported on CCA, active carbon (AC) and Al_2O_3 . All the molybdenum loadings were 12.0 wt.%, which is the minimum amount of molybdenum oxide (the precursor of molybdenum carbide) for a monolayer dispersion on the alumina and CCA supports [14]. The diffraction peaks of molybdenum carbide on the CCA and alumina supported catalysts were very weak. This implies that the molybdenum carbide was highly dispersed on these supports, which is consistent with previous work [15]. For $\text{Mo}_2\text{C}/\text{AC}$, a

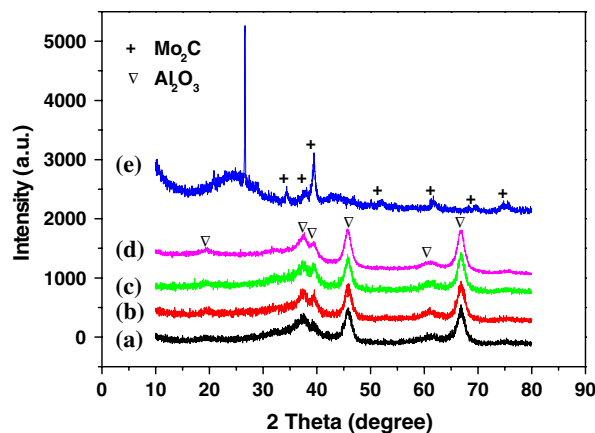


Fig. 3 XRD patterns of (a) $\text{Mo}_2\text{C}/\text{Al}_2\text{O}_3$, (b) $\text{Mo}_2\text{C}/\text{CCA-S-0.5}$, (c) $\text{Mo}_2\text{C}/\text{CCA-B-1}$, (d) $\text{Mo}_2\text{C}/\text{CCA-F}$, and (e) $\text{Mo}_2\text{C}/\text{AC}$ samples

relatively lower dispersion of molybdenum carbide was obtained, as indicated by the sharper XRD peaks of β - Mo_2C .

3.2 Hydrazine Catalytic Decomposition

The results of hydrazine decomposition on the molybdenum carbide catalysts are shown in Fig. 4. All the molybdenum carbide catalysts supported on CCA were significantly more active than that supported on conventional alumina. Especially for the CCA-S-0.5 and CCA-B-1 supported catalysts, hydrazine conversions were higher than 80% at $30\text{ }^\circ\text{C}$ and leveled off at 100% at $40\text{ }^\circ\text{C}$, in contrast with conversions as low as 12% on $\text{Mo}_2\text{C}/\text{Al}_2\text{O}_3$ at $30\text{ }^\circ\text{C}$. Thus, as supports for carbide catalysts, the CCA showed characteristics significantly superior to the conventional alumina for hydrazine decomposition. As for $\text{Mo}_2\text{C}/\text{CCA-F}$, its activity was not as high as the other two

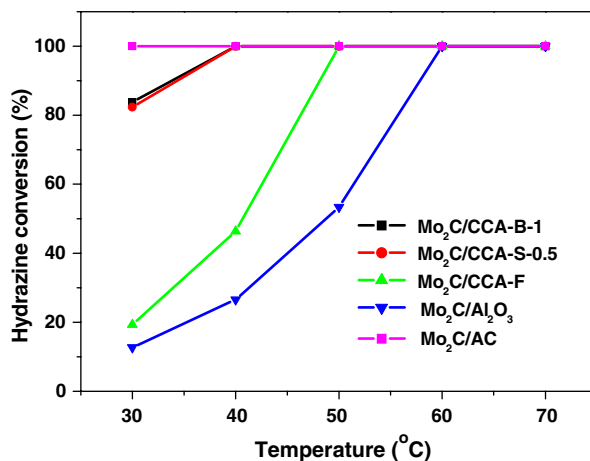


Fig. 4 Hydrazine conversions over various supported Mo_2C catalysts

CCA supported catalysts. Considering the less than 30% carbon coverage on CCA-F, which is merely a half or one third of CCA-B-1 and CCA-S-0.5, it can be inferred that carbon content played important roles in promoting the performance of the CCA supported catalysts. This is further addressed in the following section.

When molybdenum carbide was supported on the active carbon, its hydrazine conversion achieved 100% within experimental temperatures. This further demonstrates that a carbonaceous surface is advantageous over alumina alone for carbide catalysts used in hydrazine decomposition. In addition, the higher activity of AC supported molybdenum carbide might also be related to the much higher surface area of AC, which can produce considerable heat upon adsorption of N_2H_4 feedstock and consequently increase the catalytic activity.

The superior catalytic behavior of CCA supported Mo_2C catalysts probably originated from the carburization under a pure H_2 atmosphere, which would not produce much carbonaceous deposit on the carbide surface in contrast with the carburization under a CH_4/H_2 atmosphere. On the other hand, the activities might also be related to the interactions between metal and supports. The molybdenum phosphide and nitride catalysts supported on CCA-S-0.5 were prepared under hydrogen and ammonia atmospheres, respectively, and would therefore be free from any carbonaceous deposit on the active sites surface. As shown in Fig. 5, both CCA supported molybdenum nitride and molybdenum phosphide catalysts exhibited remarkably higher activities of hydrazine decomposition compared to the corresponding ones supported on alumina alone. Thus, the interaction between the carbonaceous surface and the metals was the main cause of the enhanced activities on CCA supported noble-metal like catalysts for hydrazine decomposition.

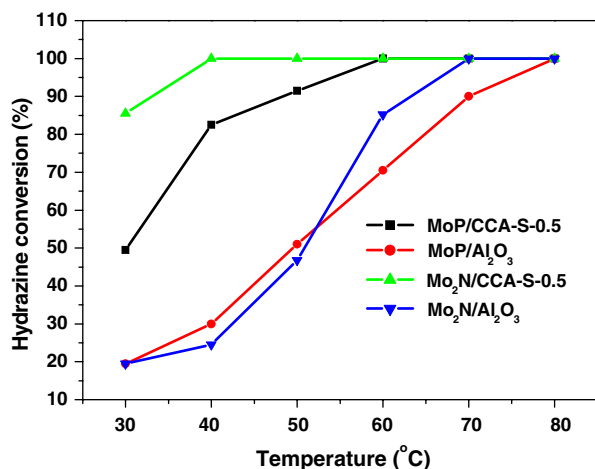


Fig. 5 Hydrazine conversions over various supported molybdenum nitride and phosphide catalysts

3.3 Influence of Carbon Contents and Carbon Sources on the Performance of CCA Supported Catalysts

CCAs with various carbon contents were used as supports for molybdenum carbide catalysts and compared in hydrazine decomposition. The texture parameters and carbon contents of these CCA supports are listed in Table 2. Referring to the content of monolayer carbon on alumina (12.4 wt%), the carbon dispersions on CCA-S-0.4, CCA-S-0.5, and CCA-S-0.6 supports varied from less than one layer, to nearly one layer, and to more than one layer of carbon, respectively. As shown in Fig. 6, the molybdenum carbide catalysts supported on CCA-S-0.5 and CCA-S-0.6 had similar higher activities for hydrazine decomposition, in contrast with that of $Mo_2C/CCA-S-0.4$. This shows that the carbon multilayer on CCA did not further improve the activity of the supported catalyst as compared with the monolayer of carbon. On the other hand, combined with the relatively low activity of $Mo_2C/CCA-F$ mentioned above, it also can be concluded that CCA support with sub-monolayer carbon presented a performance inferior to that of CCA support with monolayer carbon.

The influence of carbon contents were also examined on CCA-B supported molybdenum carbide catalysts. By

Table 2 Texture properties of CCA with different carbon contents

Supports	Temp. (°C)	S_{BET} (m ² /g)	D (nm)	S_{mic} (m ² /g)	V (cm ³ /g)	Carbon content (%)
CCA-S-0.4	800	196	4.4	20	0.25	9.3
CCA-S-0.5	800	204	4.1	17	0.24	11.4
CCA-S-0.6	800	217	3.8	24	0.23	16.1
CCA-B-1	720	177	4.3	0	0.25	9.2
CCA-B-2	720	132	3.6	0	0.15	19.8
CCA-B-3	720	99	3.6	0	0.11	25.6

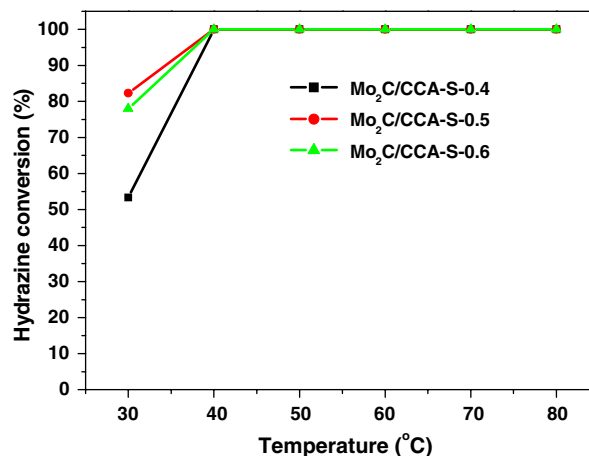


Fig. 6 Hydrazine conversions over Mo_2C catalysts supported on various CCA-S

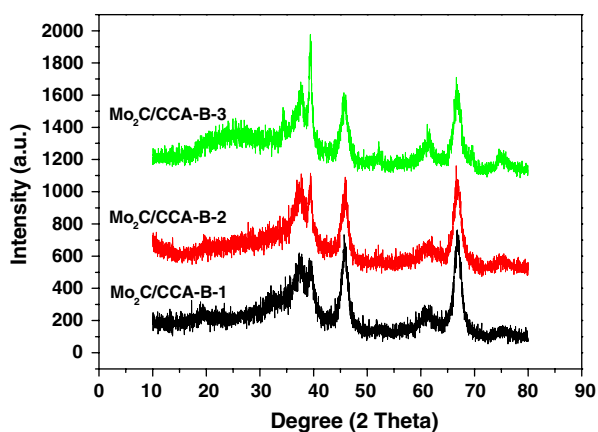


Fig. 7 XRD patterns of Mo₂C supported on various CCA-B

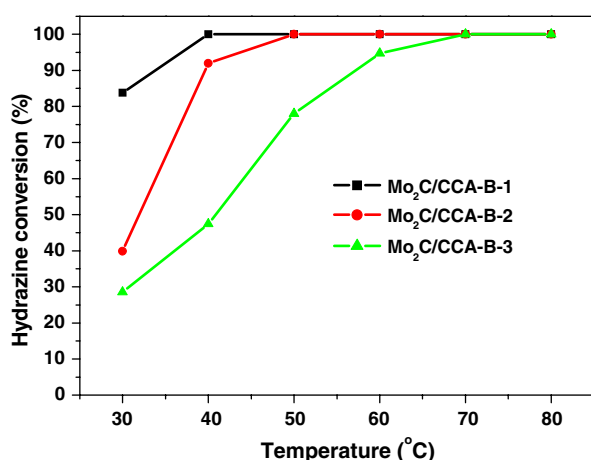


Fig. 8 Hydrazine conversions over Mo₂C catalysts supported on various CCA-B

depositing benzene vapor on alumina for a different number of hours, CCA-B were obtained with carbon contents increasing from 9.2 to 25.6 wt.%. Meanwhile, the specific surface areas of CCA-B decreased drastically from 177 to 99 m²/g and the pore volume was reduced from 0.25 to 0.11 cm³/g, indicating that the alumina pores were filled or blocked when too much carbon was deposited on CCA-B-2 and CCA-B-3. As a result, the molybdenum dispersions deteriorated on these low-surface-area CCA-B supports, which were clearly evidenced by the increase in intensity of the X-ray diffraction peaks of Mo₂C/CCA-B (Fig. 7). The hydrazine conversions as shown in Fig. 8 revealed that the highest carbon content on CCA-B-3 yielded the lowest activity for Mo₂C/CCA-B-3. This demonstrated that there is an optimal value for the carbon layer on CCA. This optimal layer appears to be the monolayer.

In addition, the carbon species on CCA and the carbon source used should also be considered because different carbon sources produce carbon with different properties. As

mentioned above, benzene more readily yielded graphite than sucrose or furfuryl alcohol did when used as a carbon source for the CCA preparation. This can be attributed to the oxygenated groups contained in the furfuryl alcohol and sucrose molecules, which left oxygen atoms in the derived carbon products even after calcination at 800 °C in an inert atmosphere. This hindered the total graphitization of carbon but resulted in the microcrystalline graphite. In contrast, benzene was more likely to form graphite by calcination due to its planar hexagonal structure and lack of oxygen atoms. For preparing molybdenum carbide catalysts, the wetness impregnation of aqueous solutions onto the supports was facilitated by the disordered edges of the microcrystalline graphite and the oxygen species contained in the carbon layer of the CCA supports, for instance CCA-S and CCA-F. However, for CCA with a high coverage of graphite, wetting the support became difficult due to the surface hydrophobicity, especially for the cases of CCA-B-2 and CCA-B-3 as we observed during the preparation. No doubt, the hydrophobic surfaces of the supports reduced the dispersions of molybdenum species and in turn decreased the catalytic activity.

4 Conclusions

Carbon covered alumina was a good support for transition metal carbide, nitride, and phosphide catalysts. With monolayer coverage of carbon on alumina, the CCA supported catalysts showed the best hydrazine decomposition performance. In other words, when the carbon deposit was in either sub-monolayer or multilayer form, the CCA supported catalysts demonstrated relatively lower activities due to the interactions between the metal and alumina or due to the low dispersions of metal on the support. Compared to the sucrose and furfuryl alcohol carbon sources, benzene more readily yielded graphite on the CCA surface. The resulting surface hydrophobicity decreased the metal dispersions and accordingly reduced the activity of the supported catalysts.

Acknowledgements The financial supports from the National Natural Science Foundation of China (NSFC) for Distinguished Young Scholars (No. 20325620) and the National Natural Science Foundation of China (No. 20573108 and No. 20303017) are gratefully acknowledged.

References

1. Levy RB, Boudart M (1973) *Science* 181:547
2. Oyama ST (1992) *Catal Today* 15:179
3. Hwu HH, Chen JG (2005) *Chem Rev* 105:185
4. Rodríguez JAJ, Cruz GM, Bugli G, Boudart M, Djéga-Mariadassou G (1997) *Catal Lett* 45:1

5. Chen XW, Zhang T, Zheng MY, Wu ZL, Wu WC, Li C (2004) *J Catal* 224:473
6. Cheng RH, Shu YY, Zheng MY, Li L, Sun J, Wang XD, Zhang T (2007) *J Catal* 249:397
7. Chen XW, Zhang T, Ying PL, Zheng MY, Wu WC, Xia LG, Li T, Wang XD, Li C (2002) *Chem Commun* 288
8. Chen XW, Zhang T, Xia LG, Li T, Zheng MY, Wu ZL, Wang XD, Wei ZB, Xin Q, Li C (2002) *Catal Lett* 79:21
9. Liang CH, Ma WP, Feng ZC, Li C (2003) *Carbon* 41:1833
10. Lin L, Lin W, Zhu YX, Zhao BY, Xie YC, Jia GQ, Li C (2005) *Langmuir* 21:5040
11. Kawabuchi Y, Kawano S, Mochida I (1996) *Carbon* 34:711
12. Ferrari AC, Robertson J (2000) *Phy Rev B* 61:14095
13. Ferrari AC, Robertson J (2001) *Phy Rev B* 64:075414
14. Xie YC, Tang Y (1990) *Adv Catal* 37:1
15. Chen XW, Zhang T, Zheng MY, Xia LG, Li T, Wu WC, Wang XW, Li C (2004) *Ind Eng Chem Res* 43:6040